

Ba₂Ti₂Fe₂As₄O: A New Superconductor Containing Fe₂As₂ Layers and Ti₂O Sheets

Yun-Lei Sun,[†] Hao Jiang,[†] Hui-Fei Zhai,[†] Jin-Ke Bao,[†] Wen-He Jiao,[†] Qian Tao,[†] Chen-Yi Shen,[†] Yue-Wu Zeng,[§] Zhu-An Xu,^{†,‡} and Guang-Han Cao^{*,†,‡}

[†]Department of Physics, [‡]State Key Lab of Silicon Materials, and [§]Center of Electron Microscope, Zhejiang University, Hangzhou 310027, China

S Supporting Information

ABSTRACT: We have synthesized a new oxypnictide, Ba₂Ti₂Fe₂As₄O, via a solid-state reaction under a vacuum. The compound crystallizes in a body-centered tetragonal lattice, which can be viewed as an intergrowth of BaFe₂As₂ and BaTi₂As₂O, thus containing Fe₂As₂ layers and Ti₂O sheets. Bulk superconductivity at 21 K is observed after annealing the as-prepared sample at 773 K for 40 h. In addition, an anomaly in resistivity and magnetic susceptibility around 125 K is revealed, suggesting a charge- or spin-density wave transition in the Ti sublattice.

The discovery of Fe-based superconductors (FeSCs)¹ has triggered enormous research activities in recent years.² So far, dozens of FeSCs in several crystallographic types have been discovered. The representative systems (with an abbreviation in numbers corresponding to their chemical compositions) are (i) FeSe (11),³ (ii) LiFeAs (111),⁴ (iii) BaFe₂As₂ (122),⁵ (iv) K_xFe_{2-y}Se₂ (122*),⁶ and (v) LaFeAsO (1111),¹ which were studied intensively.² All these compounds consist of an anti-fluorite-like Fe₂X₂ (X = As, Se) layer; therefore, the Fe₂X₂ layer is considered a crucial structural unit for Fe-based superconductivity. This point is further supported by the fact that some other compounds^{7–10} containing the same Fe₂X₂ layers (but with different block layers in between) also show superconductivity or become superconducting upon suitable chemical doping, with relatively high critical temperature (*T_c*).

To explore new FeSCs with potentially high *T_c*, therefore, a rational strategy is to build a new structure with the necessary Fe₂X₂ layers by inserting distinct block layers between them. In some oxychalcogenides and oxypnictides,^{11–22} layers of “M₂X₂O” (M = Fe, Co or Mn for X = S or Se;^{11–15} M = Ti for X = As or Sb^{16–22}) are possible candidates for the new building block. The oxypnictides with Ti₂O sheets (a reverse analogue of the CuO₂ sheets in well-known cuprate superconductors) have received considerable interest because of a possible charge-density wave (CDW) or spin-density wave (SDW) transition in the Ti sublattice.^{18–21} So, it is appealing to combine Fe₂As₂ layers with Ti₂O sheets. In this communication, we report our successful adventures in the synthesis and characterization of a new quinary oxypnictide, Ba₂Ti₂Fe₂As₄O. The crystal structure is actually an intergrowth of BaFe₂As₂ and BaTi₂As₂O²² (see Figure 1), containing both Fe₂As₂ layers and Ti₂O sheets. The new material exhibits bulk superconductivity at 21 K and a possible CDW/SDW transition around 125 K.

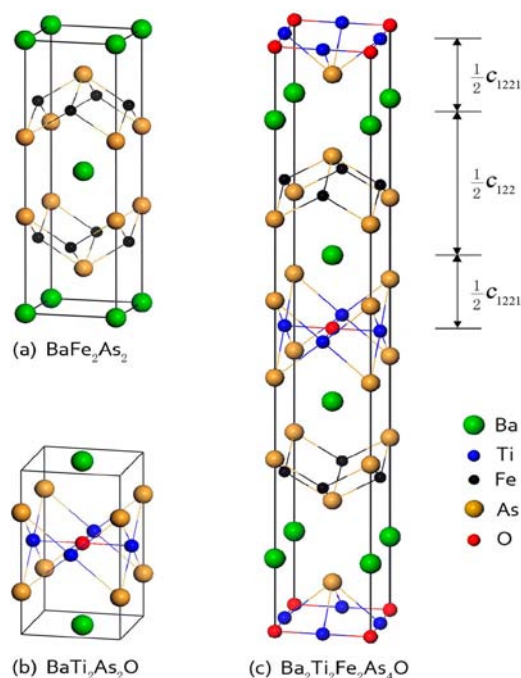


Figure 1. Intergrowth of BaFe₂As₂ (a) and BaTi₂As₂O (b) forms a new compound, Ba₂Ti₂Fe₂As₄O (c). The designed “22241” structure has space group *I4/mmm*, with an expected *c*-axis of $c_{22241} \approx (c_{122} + 2c_{1221}) \approx 27.57 \text{ \AA}$.

Polycrystalline samples of Ba₂Ti₂Fe₂As₄O were synthesized by solid-state reaction using the starting materials Ba, Ti, Fe, As, and TiO₂ with high-purity ($\geq 99.9\%$). A stoichiometric mixture of the starting materials was placed into an alumina tube and sealed in an evacuated quartz ampule. The ampule was slowly heated to 1173 K, holding for 24 h. After the first stage of reaction, the product was ground, pelletized, and sintered at 1373 K in a vacuum for 40 h, followed by cooling to room temperature after switching off the furnace. Some of the as-prepared sample was annealed at 773 K for 40 h in a vacuum. Note that all the procedures except for the ampule sealing and heating were performed in a glovebox filled with high-purity argon.

Received: May 11, 2012

Published: July 23, 2012

Powder X-ray diffraction (XRD) was carried out at room temperature using a D/Max-rA diffractometer with Cu $K\alpha$ radiation and a graphite monochromator. To confirm the structural model, high-resolution transmission electron microscopy (HRTEM) was employed using a FEI Tecnai G² F20 scanning transmission electron microscope. The detailed structural parameters were obtained by Rietveld refinement²³ using step-scan (4 s/step) data. The bond-valence sum (BVS)²⁴ was calculated on the basis of the crystallographic data refined. The electrical resistivity was measured by a standard four-terminal method with silver paste as the contact electrodes. The dc magnetic susceptibility was measured on a Quantum Design Magnetic Property Measurement System (MPMS-5).

The XRD patterns of the sample can be well indexed with a tetragonal unit cell, as shown in Figure 2a, except for several

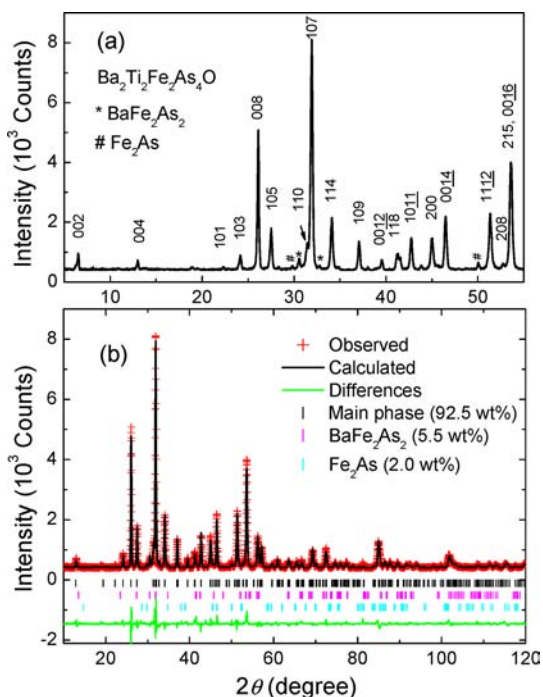


Figure 2. Indexing (a) and Rietveld refinement profile (b) of the powder X-ray diffraction for the as-prepared Ba₂Ti₂Fe₂As₄O.

small peaks coming from tiny impurities such as BaFe₂As₂, Fe₂As, and BaTi₂As₂O. Reflections appear only for the index (hkl) with $h+k+l = \text{even}$ numbers, indicating a body-centered lattice. The series of (00 l) reflections, especially for those at the lower 2θ region, point to a layered structure with $c \approx 27.3$ Å. Meanwhile, the a -axis value is close to that of BaTi₂As₂O.²² Obviously, the unit cell coincides with the structural model shown in Figure 1c. Furthermore, the HRTEM images shown in Figure 3 directly confirm the crystal structure.

Indeed, Rietveld refinement based on the intergrowth structure shows that the calculated profile well matches the experimental data. The weighted reliable factor R_{wp} and the goodness of fit S are 5.98% and 1.40, respectively, further indicating correctness of the structure.

The refined structural parameters of Ba₂Ti₂Fe₂As₄O are listed in Table 1, for comparison with those of BaFe₂As₂ and BaTi₂As₂O. The a -axis is 0.48% smaller than that of BaTi₂As₂O and 1.6% larger than that of BaFe₂As₂; thus, the Fe₂As₂ layers are more stretched within the basal planes compared with those of BaFe₂As₂. On the other hand, the Ti₂O sheets are under

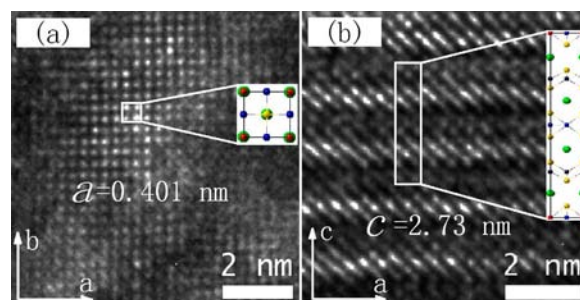


Figure 3. High-resolution transmission electron microscope images of the as-prepared Ba₂Ti₂Fe₂As₄O sample: (a) [001] zone and (b) [010] zone.

Table 1. Crystallographic Data for Ba₂Ti₂Fe₂As₄O at Room Temperature and Comparison of Some Structural Parameters with Those of the Two Related Compounds, BaFe₂As₂⁵ and BaTi₂As₂O²²

atom	x	y	z	B_{iso} (fixed)
Ba	0	0	0.1321(1)	0.1
Ti	0.5	0	0	0.5
Fe	0.5	0	0.25	0.4
As(1)	0	0	0.2996(1)	0.3
As(2)	0.5	0.5	0.0645(1)	0.3
O	0	0	0	1.0

parameter	Ba ₂ Ti ₂ Fe ₂ As ₄ O	BaFe ₂ As ₂	BaTi ₂ As ₂ O
space group	$I4/mmm$	$I4/mmm$	$P4/mmm$
a (Å)	4.0276(1)	3.9625(1)	4.047(3)
c (Å)	27.3441(4)	13.0168(3)	7.275(4)
V (Å ³)	443.57(2)	204.38(2)	119.2(3)
As height (Å)	1.356(1)	1.360(1)	n/a
As–Fe–As angle (°)	112.1(1)	111.1(1)	n/a
BVS for Ti	3.09	n/a	2.99

compression. It is also noted, for the c -axis direction, that the cell parameter c is 0.81% smaller than the expected value of 27.57 Å for the intergrowth structure. The shrink in c -axis implies enhanced interlayer chemical bonding, which stabilizes the compound.

Figure 4 shows the temperature dependence of electrical resistivity for the Ba₂Ti₂Fe₂As₄O polycrystalline samples. Both the as-prepared and the annealed samples exhibit metallic

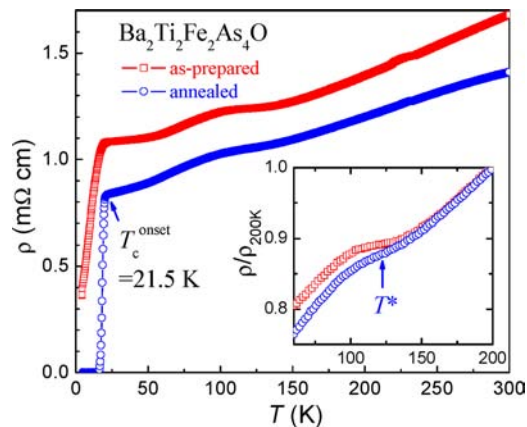


Figure 4. Temperature dependence of electrical resistivity for as-prepared and annealed Ba₂Ti₂Fe₂As₄O samples. The inset displays an expanded plot, showing an anomaly at T^* .

behavior with resistivity about $1 \text{ m}\Omega\text{-cm}$, which is comparable to that of BaFe_2As_2 ,⁵ but 1 order of magnitude larger than that of $\text{BaTi}_2\text{As}_2\text{O}$.²² The resistivity exhibits a “shoulder” at $T^* \approx 125 \text{ K}$. Below $T_c \approx 21 \text{ K}$, the resistivity decreases rapidly, and it goes to zero at 16 K for the annealed sample, indicating the existence of superconductivity in the system.

The temperature dependence of magnetic susceptibility is shown in Figure 5. Under low magnetic field, signals of

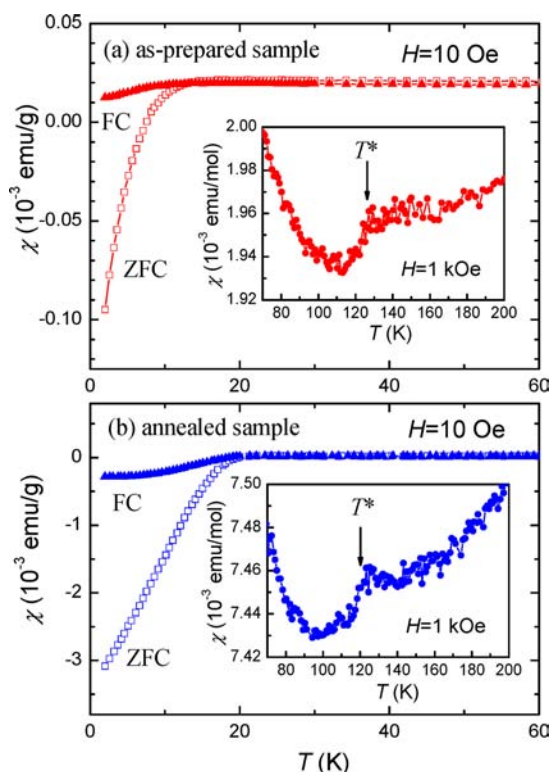


Figure 5. Temperature dependence of magnetic susceptibility for as-prepared (a) and annealed (b) $\text{Ba}_2\text{Ti}_2\text{Fe}_2\text{As}_4\text{O}$. Both zero-field-cooling (ZFC) and field-cooling (FC) processes were employed. Note that, in the insets, a higher magnetic field ($H = 1 \text{ kOe}$) was applied to trace the magnetic anomaly at T^* .

magnetic shielding (ZFC curve) and repulsion (FC curve) were observed at low temperature for both samples. The estimated shielding volume fraction at 2 K is 0.7% and 23% for the as-prepared and the annealed samples, respectively. This result corresponds with the broad and sharp transitions in the resistivity measurement. The zero resistance and relatively large shielding fraction in the annealed sample indicate that the new “22241” compound is a superconductor (note that the annealed sample keeps the 22241 phase completely, as confirmed by the XRD measurement). The “loss” of bulk superconductivity in as-prepared samples may be due to the partial occupation of Ti at the Fe site, which could destroy superconductivity.

The insets of Figure 5 clearly show a magnetization drop at $T^* \approx 125 \text{ K}$. This magnetic anomaly is not likely to be associated with the Fe_2As_2 layer which is responsible for superconductivity. Note that a similar drop in magnetic susceptibility was also observed in other compounds with $\text{Ti}_2\text{X}_2\text{O}$ block layers.^{17,19–22} In $\text{BaTi}_2\text{As}_2\text{O}$, for example, the transition occurs at a higher temperature of 200 K , which was ascribed to a CDW/SDW ordering.²² Therefore, the 125 K anomaly in the present system may be due to a suppressed

CDW/SDW transition in the $\text{Ti}_2\text{As}_2\text{O}$ block layers. Such a drop in susceptibility suggests a decrease in the density of states at the Fermi level, $N(E_F)$, possibly due to a gap opening.¹⁹ This picture may qualitatively explain the “shoulder” in resistivity shown in Figure 4 because of the loss of $N(E_F)$ for the gap opening.

The appearance of superconductivity without extrinsic doping as well as the suppression of CDW/SDW order (as compared with $\text{BaTi}_2\text{As}_2\text{O}$) in the $\text{Ti}_2\text{As}_2\text{O}$ block layers could be ascribed to the internal compression (from the BaFe_2As_2 block) and/or electron transfer from Ti-3d to Fe-3d. Electron transfer is inferred from the variations in the BVS of Ti. Compared with $\text{BaTi}_2\text{As}_2\text{O}$, the BVS value for the 22241 phase increases by 0.10 , implying that approximately 10% of Ti-3d electrons transfer to the Fe-3d states. A similar self-doping mechanism was revealed in the $\text{Sr}_2\text{VFeAsO}_3$ system, where the electrons are transferred from V to Fe.²⁵

Some structural parameters, such as the As–Fe–As angle²⁶ and the As height,²⁷ were proposed to determine the potential T_c values in the FeSCs. While the two parameters for the present material (see Table 1) are appropriate for producing superconductivity, a higher T_c would be expected by optimizing the As–Fe–As angle and/or the As height through suitable chemical doping and/or applying pressures.

To summarize, a new oxypnictide, $\text{Ba}_2\text{Ti}_2\text{Fe}_2\text{As}_4\text{O}$, containing both Fe_2As_2 layers and Ti_2O sheets was successfully synthesized. Measurements of resistivity and magnetization indicated bulk superconductivity at 21 K related to the Fe_2As_2 layers, as well as an electronic transition around 125 K possibly associated with a CDW/SDW ordering in the Ti_2O sheets. The coexistence of Fe_2As_2 -layer superconductivity and Ti_2O -sheet CDW/SDW ordering is quite rare and deserves further investigation.

■ ASSOCIATED CONTENT

📄 Supporting Information

X-ray crystallographic file (CIF). This material is available free of charge via the Internet at <http://pubs.acs.org>.

■ AUTHOR INFORMATION

Corresponding Author

ghcao@zju.edu.cn

Notes

The authors declare no competing financial interest.

■ ACKNOWLEDGMENTS

We acknowledge support from NSF of China (Contract Nos. 90922002 and 11190023), the National Basic Research Program of China (Grant Nos. 2010CB923003 and 2011CBA00103), and the Fundamental Research Funds for the Central Universities of China. We also thank Jin-Hua Hong for help with the HRTEM experiment.

■ REFERENCES

- (1) Kamihara, Y.; Hiramatsu, H.; Hirano, M.; Kawamura, R.; Yanagi, H.; Kamiya, T.; Hosono, H. *J. Am. Chem. Soc.* **2006**, *128*, 10012. Kamihara, Y.; Watanabe, T.; Hirano, M.; Hosono, H. *J. Am. Chem. Soc.* **2008**, *130*, 3296.
- (2) Johnston, D. C. *Adv. Phys.* **2010**, *59*, 803. Stewart, G. R. *Rev. Mod. Phys.* **2011**, *83*, 1589.
- (3) Hsu, F.-C.; Luo, J.-Y.; Yeh, K.-W.; Chen, T.-K.; Huang, T.-W.; Wu, P. M.; Lee, Y.-C.; Huang, Y.-L.; Chu, Y.-Y.; Yan, D.-C.; Wu, M.-K. *Proc. Natl. Acad. Sci. U.S.A.* **2008**, *105*, 14262.

- (4) Wang, X. C.; Liu, Q. Q.; Lv, Y. X.; Gao, W. B.; Yang, L. X.; Yu, R. C.; Li, F. Y.; Jin, C. Q. *Solid State Commun.* **2008**, *148*, 538.
- (5) Rotter, M.; Tegel, M.; Johrendt, D. *Phys. Rev. Lett.* **2008**, *101*, 107006.
- (6) Guo, J.; Jin, S.; Wang, G.; Wang, S.; Zhu, K.; Zhou, T.; He, M.; Chen, X. *Phys. Rev. B* **2010**, *82*, 180520(R).
- (7) Zhu, X.; Han, F.; Mu, G.; Zeng, B.; Cheng, P.; Shen, B.; Wen, H. *Phys. Rev. B* **2009**, *79*, 024516. Shirage, P. M.; Kihou, K.; Lee, C. H.; Kito, H.; Eisaki, H.; Iyo, A. *J. Am. Chem. Soc.* **2011**, *133*, 9630.
- (8) Ogino, H.; Matsumura, Y.; Katsura, Y.; Ushiyama, K.; Horii, S.; Kishio, K.; Shimoyama, J. *Supercond. Sci. Technol.* **2009**, *22*, 075008. Zhu, X.; Han, F.; Mu, G.; Cheng, P.; Wen, H. *Phys. Rev. B* **2009**, *79*, 220512(R).
- (9) Kawaguchi, N.; Ogino, H.; Shimizu, Y.; Kishio, K.; Shimoyama, J. *Appl. Phys. Exp.* **2010**, *3*, 063102.
- (10) Ni, N.; Allred, J. M.; Chen, B. C.; Cava, R. J. *Proc. Natl. Acad. Sci. U.S.A* **2011**, *108*, E1019.
- (11) Mayer, J. M.; Schneemeyer, L. F.; Siegrist, T.; Waszczak, J. V.; Dover, B. V. *Angew. Chem., Int. Ed. Engl.* **1992**, *31*, 1645.
- (12) Kabbour, H.; Janod, E.; Corraze, B.; Danot, M.; Lee, C.; Whangbo, M. H.; Cario, L. *J. Am. Chem. Soc.* **2008**, *130*, 8261.
- (13) He, J. B.; Wang, D. M.; Shi, H. L.; Yang, H. X.; Li, J. Q.; Chen, G. F. *Phys. Rev. B* **2011**, *84*, 205212.
- (14) Wang, C.; Tan, M. Q.; Feng, C. M.; Ma, Z. F.; Jiang, S.; Xu, Z. A.; Cao, G. H.; Matsubayashi, K.; Uwatoko, Y. *J. Am. Chem. Soc.* **2010**, *132*, 7069.
- (15) Ni, N.; Climent-Pascual, E.; Jia, S.; Huang, Q.; Cava, R. J. *Phys. Rev. B* **2010**, *82*, 214419.
- (16) Adam, A.; Schuster, H. -U. *Z. Anorg. Allg. Chem.* **1990**, *584*, 150.
- (17) Axtell, E. A., III; Ozawa, T.; Kauzlarich, S. M.; Singh, R. R. P. *J. Solid State Chem.* **1997**, *134*, 423.
- (18) Pickett, W. E. *Phys. Rev. B* **1998**, *58*, 4335.
- (19) Ozawa, T. C.; Kauzlarich, S. M.; Bieringer, M.; Greedan, J. E. *Chem. Mater.* **2001**, *13*, 1804.
- (20) Liu, R. H.; Tan, D.; Song, Y. A.; Li, Q. J.; Yan, Y. J.; Ying, J. J.; Xie, Y. L.; Wang, X. F.; Chen, X. H. *Phys. Rev. B* **2009**, *80*, 144516.
- (21) Liu, R. H.; Song, Y. A.; Li, Q. J.; Ying, J. J.; Yan, Y. J.; He, Y.; Chen, X. H. *Chem. Mater.* **2010**, *22*, 1503.
- (22) Wang, X. F.; Yan, Y. J.; Ying, J. J.; Li, J. Q.; Zhang, M.; Xu, N.; Chen, X. H. *J. Phys.: Condens. Matter* **2010**, *22*, 075702.
- (23) Izumi, F.; Ikeda, T. *Mater. Sci. Forum* **2000**, *321*, 198.
- (24) Brown, I. D.; Altermatt, D. *Acta Crystallogr.* **1985**, *B41*, 244. Brese, N. E.; O'Keeffe, M. *Acta Crystallogr.* **1991**, *B47*, 192.
- (25) Cao, G. H.; Ma, Z. F.; Wang, C.; Sun, Y. L.; Bao, J. K.; Jiang, S.; Luo, Y. K.; Feng, C. M.; Zhou, Y.; Xie, Z.; Hu, F. C.; Wei, S. Q.; Nowik, I.; Felner, I.; Zhang, L.; Xu, Z. A.; Zhang, F. C. *Phys. Rev. B* **2010**, *82*, 104518.
- (26) Lee, C. H.; Iyo, A.; Eisaki, H.; Kito, H.; Fernandez-Diaz, M. T.; Ito, T.; Kihou, K.; Matsuhata, H.; Braden, M.; Yamada, K. *J. Phys. Soc. Jpn.* **2008**, *77*, 083704. Zhao, J.; Huang, Q.; Cruz, C. d. I.; Li, S.; Lynn, J. W.; Chen, Y.; Green, M. A.; Chen, G. F.; Li, G.; Li, Z.; Luo, J. L.; Wang, N. L.; Dai, P. *Nat. Mater.* **2008**, *7*, 953.
- (27) Mizuguchi, Y.; Hara, Y.; Deguchi, K.; Tsuda, S.; Yamaguchi, T.; Takeda, K.; Kotegawa, H.; Tou, H.; Takano, Y. *Supercond. Sci. Technol.* **2010**, *23*, 054013.